SnO_2−In_2O_3 Nanocomposites as Semiconductor Gas Sensors for CO and NO_x Detection

Justin T. McCue[†] and Jackie Y. Ying*[,†,‡]

Department of Chemical Engineering, Massachusetts Institute of Technology, Cambridge, Massachusetts 02139-4307, and Institute of Bioengineering and Nanotechnology, 31 Biopolis Way, The Nanos, Singapore 138669, Singapore

Received July 25, 2006. Revised Manuscript Received October 30, 2006

Gas sensors based upon semiconductor metal oxides provide for the safe detection of toxic gases, such as carbon monoxide in households, natural gas in coal mines, and ethanol in fermentation processes. However, they still suffer from several limitations, such as long-term response reproducibility and gas sensitivity and selectivity. The need for thermally stable gas sensor materials that possess ultrahigh sensitivity and selectivity, often in the presence of other adsorbing gases, presents a major challenge. In this work, we have synthesized tin−indium oxide (SnO_2−In_2O_3) nanocomposites that exhibited superior thermal stability against grain growth. Through the introduction of metal clusters and oxide surface coatings, the SnO_2−In_2O_3 nanocomposites achieved superb sensitivity for both reducing and oxidizing gases. Our synthesis method provided an inexpensive and flexible wet-chemical route toward tailoring semiconductor metal oxide nanocomposites for the selective and reproducible detection of toxic or combustible gases at parts per million levels.

1. Introduction

SnO_2, an n-type semiconductor, has proven to be a highly sensitive material for the detection of both reducing gases (e.g., CO, CH_4, and H_2) and oxidizing gases (e.g., NO_x).[1−5] Unfortunately, several problems exist with currently available semiconductor sensors based on SnO_2 and other single-component oxides; they are simultaneously sensitive to too many gases.[5,6] Thus, commercially available semiconductor sensors often give an undesired signal when an inert gas is present in the environment. Existing gas sensors also tend to lack long-term stability; they require a fairly high operating temperature, and the microstructural changes over time lead to reduced sensitivity. The resistance of these devices is often irreversible and irreproducible. Semiconductor sensors also involve long response and recovery times. These various drawbacks present interesting challenges that would require better design of sensor materials, which would involve treating advanced semiconductor sensor systems not only as electronic materials, but also as structural and catalytic materials. This implies that we should consider the composition and microstructure of sensors in terms of providing superior thermal and long-term stability, as well as electronic and chemical reactivity.

Recent studies have shown that the addition of a secondary component, in the form of surface additives or dopants, could be used to inhibit SnO_2 grain growth at calcination temperatures $\leq$700 °C as well as enhance SnO_2 gas sensor performance, especially in the presence of reducing gases.[2,7] In_2O_3 is a promising candidate since it shows good sensitivity for the detection of oxidizing gases, such as NO_x and O_3, as a single-component oxide.[8] Thus, when SnO_2 and In_2O_3 are combined as a nanocomposite, the resulting system has the potential for tunable sensitivity and selectivity for different gases. The nanocrystals of the different oxide components may further act to suppress grain growth of the overall system, providing for excellent thermal stability, which would be highly desirable for reproducible, long-term gas-sensing performance. Through the incorporation of dopants and surface additives, superb sensitivity and selectivity for the detection of parts per million levels of both reducing gas (CO) and oxidizing gases (NO and NO_2) were achieved by SnO_2−In_2O_3 nanocomposites.

2. Experimental Section

SnO_2−In_2O_3 powders were prepared by precipitating an aqueous solution of $SnCl_4 \cdot 6H_2O$ (Alfa Aesar, 99.99%) and $InCl_3 \cdot H_2O$ (Alfa Aesar, 99.9%) induced by dropwise addition of ammonium hydroxide (Mallinckrodt). The total salt concentration ($Sn^{4+} + In^{3+}$) was varied from 0.005 to 0.5 M, while the final solution pH was varied between 2 and 10. The solution pH was measured with an Orion 420C pH meter. Following precipitation, the slurry was aged for 24 h, centrifuged, washed three times with distilled H_2O, dried

* To whom correspondence should be addressed. E-mail: jyying@ibn.a-star.edu.sg.
† Massachusetts Institute of Technology.
‡ Institute of Bioengineering and Nanotechnology.

(1) Ihokura, K.; Watson, J. *The Stannic Oxide Gas Sensor - Principles and Applications*; CRC Press: Boca Raton, FL, 1994.
(2) Xu, C.; Tamaki, J.; Miura, N.; Yamazoe, N. *Sens. Actuators, B* **1991**, *3*, 147.
(3) Williams, G.; Coles, G. S. V. *J. Mater. Chem.* **1998**, *8*, 1657.
(4) Williams, G.; Coles, G. S. V. *Sens. Actuators, B* **1993**, *15*−*16*, 349.
(5) Morrison, R. S. *Sens. Actuators* **1982**, *2*, 329.
(6) Van Gelovan, P.; Honore, M.; Roggen, J.; Leppavuori, S.; Rantala, T. *Sens. Actuators, B* **1991**, *4*, 185.
(7) Wu, N.; Wang, S.; Rusakova, I. *Science* **1999**, *285*, 1375.
(8) Gurlo, A.; Ivanovskaya, M.; Bârsan, N.; Schweizer-Berberich, M.; Weimar, U.; Göpel, W.; Diéguez, A. *Sens. Actuators, B* **1997**, *44*, 327.

10.1021/cm0617283 CCC: $37.00
Published on Web 02/09/2007

at 120 °C, and ground in a mortar and pestle to break up any weak agglomerates. The dried powder was calcined in air at 400−1000 °C for 6 or 40 h (ramp 3 °C/min).

The $SnO_2-In_2O_3$ nanocomposites could also be modified through the introduction of 0−10 wt % metal dopants or oxide surface deposits. For "doping" of the $SnO_2-In_2O_3$ nanocomposites, ammonium, chloride, or nitrate salts of the desired cations were introduced to the precursor solution prior to precipitation. For "coating" of the $SnO_2-In_2O_3$ nanocomposites, nitrate or chloride salts of the desired cations were added to the aging mixture 24 h after the $SnO_2-In_2O_3$ precipitation. Following addition of the dopant or coating, the modified $SnO_2-In_2O_3$ nanocomposites were aged for 24 h, dried, ground, and calcined, as described earlier.

The surface area of the $SnO_2-In_2O_3$ powders was determined from nitrogen adsorption analysis by the five-point BET (Brunauer−Emmett−Teller) method on a Micromeritics ASAP 2000 gas adsorption analyzer. Phase identification was performed by powder X-ray diffraction (XRD) using a Siemens D5000 $\theta-\theta$ diffractometer (45 kV, 40 mA, Cu Kα). The crystallite size was obtained from the broadening analysis of the SnO_2(110) diffraction peak ($2\theta = 26.6°$) using Scherrer's method, corrected for instrumental line broadening. The lattice parameters of the nanocomposites were obtained from XRD analysis with Si powder as an internal standard.

High-resolution transmission electron microscopy (HR-TEM) was performed on a JEOL 2010 microscope (200 kV). X-ray photoelectron spectroscopy (XPS) measurements were obtained on an ESCA ESX-100 spectrometer. The binding energy was calibrated internally by the C1s line position.

Samples for temperature-programmed desorption (TPD) studies were pretreated in air at 550 °C for 6 h to remove surface adsorbates. Following cooling to room temperature in air, the samples were exposed to 1000 ppm NO in air for 6 h. Desorption of adsorbed species was performed during heating (ramp 2 °C/min) in flowing helium at atmospheric pressure and was analyzed with a Hewlett-Packard 6890 gas chromatograph with a mass-selective detector.

For gas sensitivity studies, the calcined nanocomposite powders were cold isostatically pressed into pellets (10 mm in diameter, 2 mm in thickness) at 30000 psi. Electrical leads were mounted on the surface of the pellet using silver paste. The device was enclosed in a quartz tube, which was heated to 50−300 °C in a tube furnace (Lindberg Blue). Prior to sensor testing, the device was heated to 300 °C for 24 h. CO, NO, NO_2, and air flows were then introduced by independent mass flow controllers (MKS). A constant current (1.0 μA) was applied across the pellet, and the electrical resistance of the pellet was measured in air (R_{air}) and in the presence of the target gases (CO, NO, and NO_2) in air (R_g). The CO concentration was varied from 0 to 1000 ppm, while the NO and NO_2 concentrations were varied from 0 to 20 ppm.

3. Results and Discussion

3.1. Structural Characterization of $SnO_2-In_2O_3$ Nanocomposites. By manipulating the Sn/In cationic ratio, metal chloride concentrations, and solution pH, nanocrystalline $SnO_2-In_2O_3$ powders were derived with superior thermal stability compared with pure SnO_2 or In_2O_3 nanocrystals. For example, nanocomposites synthesized with a Sn/In cationic ratio of 3 (75% SnO_2−25% $InO_{1.5}$) and a solution pH of 8.0 possessed ultrafine SnO_2 grains of ∼3 nm and a BET surface area of 93 m^2/g upon calcination to 600 °C. In contrast, pure SnO_2 nanocrystals underwent substantial grain growth to 19 nm and a reduction in surface area to 19 m^2/g after heat treatment at 600 °C. Upon calcination to 800 °C, the grain size of pure SnO_2 increased to 38 nm, which was

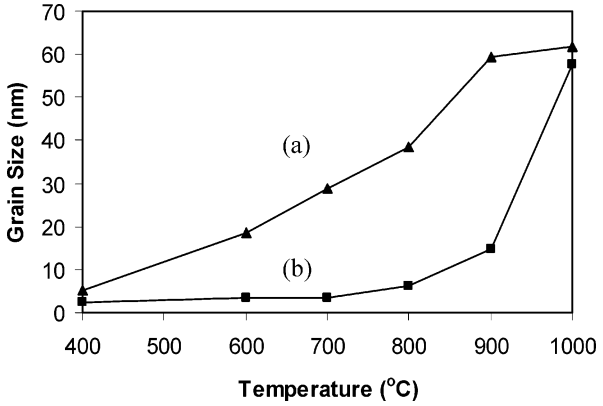

Figure 1. SnO_2 grain size for (a) pure SnO_2 and (b) 75% SnO_2−25% $InO_{1.5}$ calcined in air for 6 h at the temperature specified.

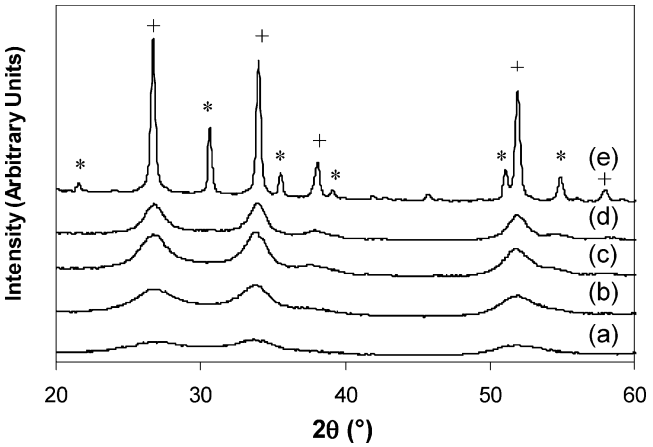

Figure 2. XRD patterns of 75% SnO_2−25% $InO_{1.5}$ calcined at (a) 400 °C, (b) 600 °C, (c) 700 °C, (d) 800 °C, and (e) 1000 °C in air for 6 h. SnO_2 (+) and In_2O_3 (*) peaks are denoted.

over 6 times larger than that of the 75% SnO_2–25% $InO_{1.5}$ nanocomposite (Figure 1). Through nanocomposite processing, In_2O_3 was able to dramatically suppress SnO_2 grain growth and loss in surface area in heat treatments up to 900 °C.

The Sn/In cationic ratio played a critical role in the thermal stability and phase composition of the binary oxide. Besides possessing ultrafine SnO_2 crystallites, 75% SnO_2−25% $InO_{1.5}$ maintained a single SnO_2 phase at temperatures ≤800 °C (Figure 2). A distinct In_2O_3 phase only emerged upon heat treatment at 1000 °C.

HR-TEM confirmed the SnO_2 crystallinity and ultrafine grain size for the 75% SnO_2−25% $InO_{1.5}$ nanocomposite. At 600 °C, the nanocomposite consisted of particles of fully crystalline SnO_2 (Figure 3b). The ultrafine SnO_2 crystallite size observed in HR-TEM (∼3 nm) was in good agreement with that obtained by XRD analysis. These SnO_2 crystallites did not undergo grain growth even after calcination for 40 h at 600 °C. After calcination at 800 °C (Figure 3c,d), SnO_2 crystallites of ∼6 nm were obtained. Crystalline In_2O_3 phases were not observed in the HR-TEM images, confirming that In_2O_3 was present as an amorphous phase in this nanocomposite system calcined to ≤800 °C.

Nanocomposites with 0−35 cation % In were examined in further detail to determine the nature of this secondary component. XRD analysis was carried out assuming a rutile-type structure for these SnO_2-based nanocomposites. The

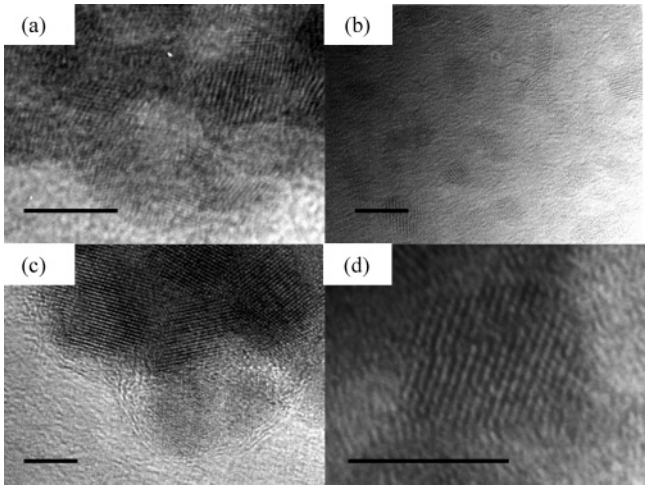

Figure 3. HR-TEM micrographs of the 75% SnO_2−25% $InO_{1.5}$ nanocomposite calcined to (a) 400 °C, (b) 600 °C, and (c, d) 800 °C in air for 6 h. The scale bars shown are 5 nm.

Table 1. Unit Cell Parameters for SnO_2−In_2O_3 Nanocomposites Containing 0−35 Cation % In[a]

[In] (cation %)	*a* (Å)	*c* (Å)	SnO_2 grain size (nm)
0	4.738	3.187	38
2	4.735	3.195	19
5	4.737	3.190	14
15	4.738	3.197	7.5
25	4.738	3.200	6.0
35	4.738	N/A	6.0

[a] Materials were calcined at 800 °C in air for 6 h. The uncertainties in the unit cell parameters *a* and *c* were ±0.001 and ±0.005 Å, respectively.

calculated unit cell parameters are shown in Table 1. For nanocomposites containing 0−25 cation % In, the changes in the *a* and *c* parameters were negligible. This suggested that In was not introduced as a dopant into the SnO_2 structure since the considerable difference in the ionic radii of In^{3+} and Sn^{4+} (0.80 and 0.69 Å, respectively[9]) would have led to observable changes in *a* and *c* if In ions were substituted into the SnO_2 lattice. The solubility of $InO_{1.5}$ in SnO_2 has been reported to be ∼7 mol %,[10,11] so the large amount of In (≤25 cation %) might have existed as a highly dispersed In_2O_3 amorphous coating on the SnO_2 nanocrystallites. A secondary In_2O_3 phase did form at 800 °C for the nanocomposite containing 35 cation % In, again with no marked changes in the SnO_2 lattice parameters.

XPS measurements were used to determine the electronic states of Sn and In in the oxide nanocomposites. The Sn3d, In3d, and O1s XPS spectra were obtained for SnO_2−$InO_{1.5}$ nanocomposites with 0−35 cation % In, as well as for a physical mixture of 75% SnO_2 and 25% $InO_{1.5}$. Table 2 shows the electron binding energies of $Sn3d_{5/2}$, $In3d_{5/2}$, and $O1s_{1/2}$ for the different materials. The measured binding energy for pure SnO_2, 486.4 eV, corresponded to the reported value for Sn^{4+} in SnO_2.[12] A significant positive chemical shift of 0.5−0.7 eV in the $Sn3d_{5/2}$ peak relative to the peak for pure SnO_2 was observed for the SnO_2−$InO_{1.5}$ nanocomposites containing 5−35 cation % In. This suggested that electronic interactions existed between Sn and In in the nanocomposites and that the degree of interaction did not vary substantially for systems with 5−35 cation % In. In contrast, an insignificant chemical shift relative to the peak for pure SnO_2 was noted in the physical mixture of 75% SnO_2 and 25% $InO_{1.5}$.

Table 2. XPS Analysis of SnO_2 and In_2O_3 Nanocrystals, a Physical Mixture of SnO_2 and In_2O_3, and Various SnO_2−$InO_{1.5}$ Nanocomposites[a]

	binding energy (eV)		
sample	$Sn3d_{5/2}$	$In3d_{5/2}$	$O1s_{1/2}$
SnO_2	486.4		534.9
In_2O_3		445.6	535.5
mixture of 75% SnO_2 and 25% $InO_{1.5}$	486.6	445.7	535.0
95% SnO_2−5% $InO_{1.5}$	486.9	445.7	535.4
85% SnO_2−15% $InO_{1.5}$	487.1	445.6	535.4
75% SnO_2−25% $InO_{1.5}$	487.0	445.6	535.4
65% SnO_2−35% $InO_{1.5}$	487.0	445.7	535.3

[a] The uncertainty in the binding energy measurements was ±0.1 eV.

Negligible shifts in binding energy were noted in the $In3d_{5/2}$ peak of the SnO_2−$InO_{1.5}$ nanocomposites relative to pure In_2O_3 (Table 2). The measured binding energies for $In3d_{5/2}$ in the compositions examined (445.6−445.7 eV) were similar to that reported for In^{3+} in In_2O_3 (445.6 eV).[13] We note that a shift in the $In3d_{5/2}$ signal due to electronic interaction between In_2O_3 and SnO_2 might not be detectable, as the binding energy shift for the In^{3+}-to-In^{1+} transition was reported to be only about −0.1 eV.[13]

A positive $O1s_{1/2}$ peak shift of 0.4−0.5 eV relative to the peak for pure SnO_2 was also noted for the various SnO_2−$InO_{1.5}$ nanocomposites. In contrast, a significant chemical shift was not measured for the $O1s_{1/2}$ peak in the physical mixture of 75% SnO_2 and 25% $InO_{1.5}$. The positive $Sn3d_{5/2}$ and $O1s_{1/2}$ peak shifts for the SnO_2−In_2O_3 composites suggested a decrease in the electron-depleted surface layer (space charge layer), relative to the pure component (SnO_2), which could potentially affect the gas-sensing properties of the material.

3.2. Gas-Sensing Properties. *3.2.1. SnO_2−In_2O_3 Nanocomposites*. The sensitivity of the SnO_2−$InO_{1.5}$ nanocomposites to CO, NO, and NO_2 gases was examined over a range of operating temperatures after calcination to 700 °C. CO sensitivity (K_{CO}) was defined as the ratio of the sensor resistance in air (R_{air}) to that in an air−CO mixture (R_{CO}), while NO_x sensitivity (K_{NO_x}) was defined as the ratio of the sensor resistance in an air−NO_x mixture (R_{NO_x}) to that in air. The 75% SnO_2–25% $InO_{1.5}$ nanocomposite had the highest sensitivities (28 and 5, respectively) to 1000 ppm CO and 20 ppm NO_2 when calcined to 700 °C. In contrast, pure nanocrystalline SnO_2 prepared in a similar fashion had CO and NO_2 sensitivities of 11 and 3, respectively. Enhanced gas sensitivities could be attributed to the much smaller SnO_2 grain size (3.4 nm) in the 75% SnO_2−25% $InO_{1.5}$ nanocomposite compared to pure SnO_2 (29 nm) (see Figure 1). Nanocomposites containing ≥50 cation % In had a low sensitivity of <2 to CO and NO_2 as pure In_2O_3 nanocrystals.

(9) Yanagisawa, K.; Udawatte, C. P. *J. Mater. Res.* **2000**, *156*, 1404.
(10) Enoki, H.; Echigoya, J.; Suto, H. *J. Mater. Sci.* **1991**, *2615*, 4110.
(11) Frank, G.; Brock, L.; Bausen, H. D. *J. Cryst. Growth* **1976**, *36*, 179.
(12) Wagner, C. D.; Biloen, P. *Surf. Sci.* **1973**, *35*, 82.
(13) McGuire, G. E.; Schweitzer, G. K.; Carlson, T. A. *Inorg. Chem.* **1973**, *12*, 2450.

Table 3. CO Sensitivity and SnO_2 Grain Size as a Function of Calcination Temperature for SnO_2 and 75% SnO_2−25% $InO_{1.5}$[a]

	CO sensitivity (K_{CO})		SnO_2 grain size (nm)	
calcination temp (°C)	SnO_2	75% SnO_2−25% $InO_{1.5}$	SnO_2	75% SnO_2−25% $InO_{1.5}$
500	38	5.5	10	amorphous
600	29	16	19	3.3
700	5.5	15	29	3.4
800	1.9	4.5	38	6.3

[a] The materials were exposed to 500 ppm CO at 200 °C.

The decreased gas sensitivity with nanocomposites containing ≥25 cation % In suggested SnO_2 was the major sensing component in the SnO_2−$InO_{1.5}$ nanocomposites.

The effect of calcination temperature on CO sensitivity was examined for 75% SnO_2−25% $InO_{1.5}$ and pure SnO_2, the two compositions possessing the highest gas sensitivities (Table 3). The 75% SnO_2−25% $InO_{1.5}$ nanocomposite displayed a lower sensitivity for CO detection than pure SnO_2 for calcination temperatures ≤600 °C. The lower CO sensitivity may have been caused by an electronic interaction between Sn and In in the nanocomposite, as indicated by a positive shift in the $Sn3d_{5/2}$ and $O1s_{1/2}$ electron binding energies (see section 3.1). The positive shift indicated a decrease in the space charge layer for Sn, which has been shown to decrease the sensitivity for the detection of reducing gases, such as CO.[3,7,16−18]

For the 75% SnO_2−25% $InO_{1.5}$ nanocomposite, a sufficient degree of crystallinity was required to attain the desired electronic properties necessary for gas sensor applications.[2,3,14,15] The 75% SnO_2−25% $InO_{1.5}$ nanocomposite was not fully crystalline at a calcination temperature of 500 °C, which explained the relatively low CO sensitivity of 5.5. A maximum sensitivity of 16 for 500 ppm CO was achieved for the nanocomposite at a calcination temperature of 600 °C and did not significantly decrease until calcination to 800 °C. The loss in gas sensitivity at elevated temperatures was due to an increase in grain size for both the pure SnO_2 and the nanocomposite.

3.2.2. Doped SnO_2−In_2O_3 Nanocomposites. The addition of surface-active deposits and dopants has proven to greatly improve gas detection, as well as to reduce operating temperature requirements in semiconductor gas sensors.[3,7,16,17] Previous research has shown that the doping of noble metals and +3 valence cations into SnO_2 could give rise to significantly improved CO sensitivity[2] due to an increase in the space charge layer thickness of SnO_2. Use of noble metals (e.g., Pt, Pd, and Au) as dopants could also enhance the catalytic properties of SnO_2 for CO oxidation,[18] improving the CO sensor performance.

In our study, the method of additive introduction, as well as the nature and loading of additives, was examined for the optimized oxide nanocomposite containing 75% SnO_2 and 25% $InO_{1.5}$. Additives introduced prior to the SnO_2−$InO_{1.5}$ precipitation were considered as "dopants", while those added following precipitation were regarded as surface oxide deposits or "coatings". The method of additive introduction had a dramatic effect on the gas-sensing properties of the 75% SnO_2−25% $InO_{1.5}$ nanocomposite.

Table 4. XPS Analyses and CO Sensitivities of Pure and Au- and Pt-Doped 75% SnO_2−25% $InO_{1.5}$ Nanocomposites Calcined to 600 °C[a]

	binding energy (eV)		
dopant	$Sn3d_{5/2}$	$O1s_{1/2}$	CO sensitivity (R_{air}/R_{CO})
	487.0	535.4	11
2 wt % Au	487.2	535.6	480
2 wt % Pt	486.3	534.7	290
4 wt % Pt	486.3	534.7	6200
6 wt % Pt	486.6	535.1	1100
10 wt % Pt	486.7	535.1	520

[a] The materials were exposed to 1000 ppm CO in air at 50 °C. The uncertainty in the binding energy measurements was ±0.1 eV.

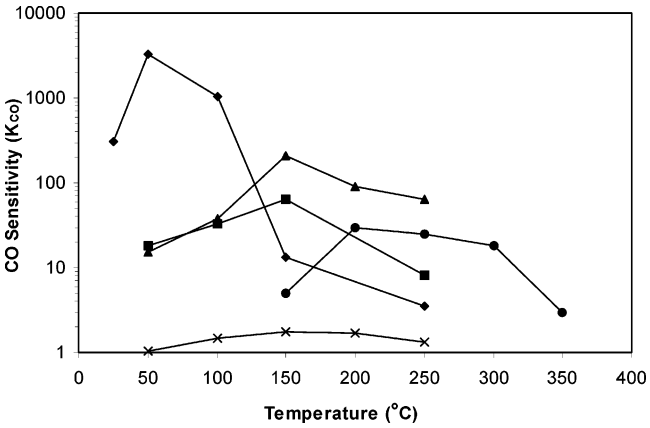

Figure 4. CO sensitivity for (×) pure SnO_2, (●) 2 wt % Au-doped SnO_2, (■) 4 wt % Pt-doped SnO_2, (▲) the 2 wt % Au-doped 75% SnO_2−25% $InO_{1.5}$ nanocomposite, and (◆) the 4 wt % Pt-doped 75% SnO_2−25% $InO_{1.5}$ nanocomposite. The 600 °C-calcined materials were exposed to 500 ppm CO in air.

The doped nanocomposites were calcined at 600 °C, which was found to be the optimal calcination temperature as it ensured SnO_2 crystallization in the nanocomposites without significant grain growth, thereby maximizing gas sensitivity. When introduced as a dopant, Au and Pt substantially increased the CO sensitivity of 75% SnO_2−25% $InO_{1.5}$ (Table 4). Sensitivity toward CO in air was increased from 11 to 480 upon doping of 2 wt % Au. An optimal Pt loading of 4 wt % was found to dramatically improve the sensitivity toward 1000 ppm CO to 6200 for the 75% SnO_2−25% $InO_{1.5}$ nanocomposite at 50 °C. This compared favorably to sensitivities of ∼3000 for 10000 ppm CO at 100 °C[15] and ∼1900 for 500 ppm CO at 20 °C,[7] reported for the Pt- and Pd-doped SnO_2 systems, respectively.

The optimized Pt-doped nanocomposite was a highly sensitive CO detector over an operating temperature range of 25−150 °C and displayed an impressive improvement in CO detection compared to conventional SnO_2-based sensor materials (Figure 4). Four weight percent Pt-doped SnO_2 prepared in a similar fashion had a maximum CO sensitivity of 63 at 150 °C, which was ∼52 times lower than that achieved by the 4 wt % Pt-doped 75% SnO_2−25% $InO_{1.5}$

(14) Xu, C.; Tamaki, J.; Miura, N.; Yamazoe, N. *Denki Kagaku* **1990**, *58*, 1143.
(15) Williams, G.; Coles, G. S. V. *MRS Bull.* **1999**, *24*, 25.
(16) Machida, M. *Catalysis*; The Royal Society of Chemistry: Cambridge, 2000; Vol. 15, p 73.
(17) Yamazoe, N.; Kurokawa, Y.; Seiyama, T. *Sens. Actuators* **1983**, *4*, 283.
(18) Haruta, M.; Tsubota, S.; Kobayashi, T.; Kageyama, H.; Genet, M. J.; Delmon, B. *J. Catal.* **1993**, *144*, 190.

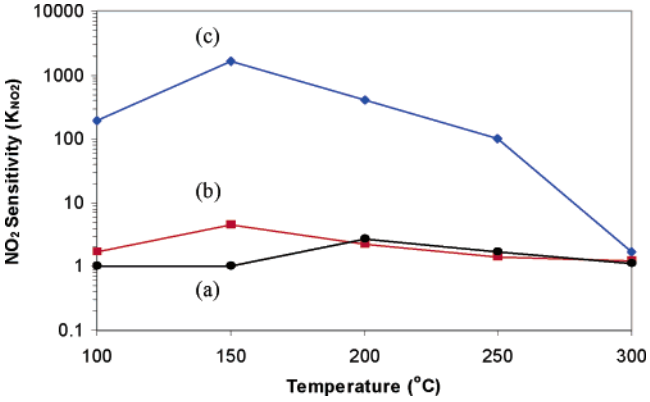

Figure 5. NO_2 sensitivity for (a) SnO_2, (b) Al_2O_3-coated SnO_2, and (c) the Al_2O_3-coated 75% SnO_2−25% $InO_{1.5}$ nanocomposite. The atmosphere consisted of 1 ppm NO_2 in air. The samples were calcined to 600 °C; samples b and c contained 2 wt % Al.

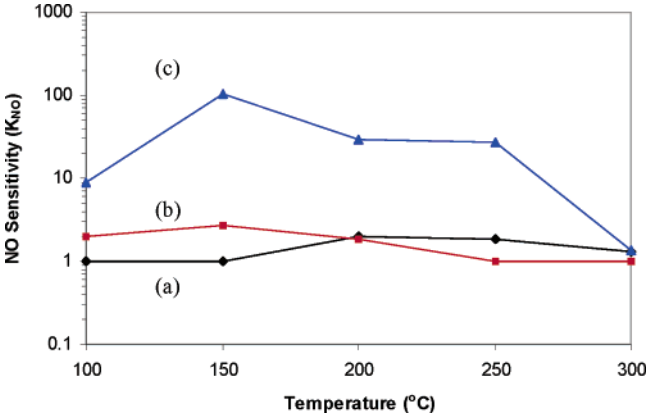

Figure 6. NO sensitivity for (a) SnO_2, (b) Al_2O_3-coated SnO_2, and (c) the Al_2O_3-coated 75% SnO_2−25% $InO_{1.5}$ nanocomposite. The atmosphere consisted of 1 ppm NO in air. The samples were calcined to 600 °C; samples b and c contained 2 wt % Al.

nanocomposite, which has a maximum CO sensitivity of 3300 at 50 °C.

Four weight percent Pt-doped 75% SnO_2−25% $InO_{1.5}$ also showed repeatable and consistent responses to 50 ppm pulses of CO. At 50 °C, it has response and recovery times of ∼22 and ∼40 min, respectively. These values were highly temperature-dependent and were significantly reduced at higher operating temperatures. Response and recovery times of ∼2 and ∼7 min were achieved at 250 °C, which were much faster that those reported for other SnO_2-based systems.[19]

3.2.3. Coated SnO_2−In_2O_3 Nanocomposites. Metal oxides such as Al_2O_3, Ga_2O_3, CeO_2, NiO, and Cr_2O_3, which are known to be effective NO_x catalysts[21−23] and/or adsorbents,[24−25] were introduced in this study as surface coatings to nanocomposite sensors to enhance the NO_x adsorption and sensitivity. In particular, the NO_2 sensitivity of 75% SnO_2−25% $InO_{1.5}$ was dramatically improved from 6.0 to 1600 with the introduction of Al_2O_3 as a surface oxide coating.

Sberveglieri et al. reported a large increase in the NO_x sensitivity of SnO_2 from 1 to ∼80 using a mechanical mixture of 10 wt % Al_2O_3 and 90 wt % SnO_2. The effect was attributed to enhanced NO_x adsorption on the SnO_2 surface.[25,26] In this work, remarkable enhancement in NO_x-sensing properties could be attributed to nanocomposite processing, which offered an ultrafine grain size for 75% SnO_2−25% $InO_{1.5}$ and a greater dispersion of Al_2O_3 than that achievable in a mechanical mixture of Al_2O_3 and SnO_2.

Al_2O_3-coated 75% SnO_2−25% $InO_{1.5}$ also demonstrated remarkable sensitivities to 1 ppm NO_2 (Figure 5) and NO (Figure 6) over a temperature range of 100−300 °C. Its maximum NO_2 and NO sensitivities (1600 and 104, respectively) were superior to those of pure and Al_2O_3-coated SnO_2. The optimal operating temperature for maximizing NO_2 and NO sensitivities was 150 °C.

The effect of the Al_2O_3 loading level on NO_2 and NO sensitivity was examined to determine the optimal loading. A loading of 2 wt % Al gave rise to the highest sensitivities for both NO_2 and NO. At an operating temperature of 150 °C, the Al_2O_3-coated nanocomposite (containing 2 wt % Al) had sensitivities of 1600 and 110 for 1 ppm NO_2 and NO, respectively. In contrast, Al_2O_3-coated SnO_2 prepared in a similar fashion (containing 2 wt % Al) possessed NO_2 and NO sensitivities of 4.5 and 2.7, respectively. The use of high Al loadings (≥10 wt %) resulted in complete loss of NO_x sensitivity, which was to be expected as Al_2O_3 possessed no gas-sensing properties as a single component.

The Al_2O_3-coated 75% SnO_2−25% $InO_{1.5}$ nanocomposite (containing 2 wt % Al) displayed reproducible responses to pulses of NO_2 and NO. At 150 °C, the sensor had NO_2 response and recovery times of 28 and 60 min, respectively. At 200 °C, it showed response and recovery times of 6 and 36 min, respectively, which were faster than the values reported for pure SnO_2[20] and 10 wt % Al_2O_3−90 wt % SnO_2.[25] We note that the response and recovery times for NO_x detection would decrease significantly for the Al_2O_3-coated 75% SnO_2−25% $InO_{1.5}$ nanocomposite at higher operating temperatures (e.g., 3 and 20 min, respectively, at 250 °C).

3.3. Gas-Sensing Mechanism of Modified SnO_2−In_2O_3 Nanocomposites. XPS, XRD, and TPD studies were used to examine the nature of interaction between the additives and the semiconductor nanocomposite oxide sensors. Two types of interactions have been proposed and may be distinguished by XPS analysis.[17,27−31] Chemical sensitization involves the adsorption of the target gas on the additive surface followed by migration (or spillover) to the semicon-

(19) Chiorino, A.; Ghiotti, G.; Carotta, M. C.; Martinelli, B. *Sens. Actuators, B* **1998**, *47*, 205.
(20) Chen, L.; Horiuchi, T.; Mori, T. *Catal. Lett.* **2001**, *72*, 71.
(21) Shimizu, K.; Takamatsu, M.; Nishi, K.; Yoshida, H.; Satsuma, A.; Tanaka, T.; Yoshida, S.; Hattori, T. *J. Phys. Chem. B* **1999**, *103*, 1542.
(22) Auroux, A.; Sprinceana, D.; Gervasini, A. *J. Catal.* **2000**, *195*, 140.
(23) Kugler, E. L.; Kadet, A. B.; Gryder, J. W. *J. Catal.* **1976**, *41*, 72.
(24) Solymosi, F.; Kiss, J. *J. Catal.* **1978**, *54*, 42.
(25) Sberveglieri, G.; Groppelli, S.; Nelli, P. *Sens. Actuators* **1990**, *1*, 79.
(26) Sberveglieri, G.; Faglia, G.; Groppelli, S.; Nelli, P. *Sens. Actuators, B* **1992**, *8*, 79.
(27) Yamazoe, N.; Kurokawa, Y.; Seiyama, T. *Proceeding of the International Meeting on Chemical Sensors*; Kodansha: Tokyo; Elsevier: Amsterdam, 1983; p 35.
(28) Bond, G. C.; Fuller, M. J.; Molloy, L. *Proceedings of the 6th International Congress on Catalysis*; Elsevier: London, 1976; p 356.
(29) Tonomura, S.; Matsuoka, T.; Yamamoto, N.; Tsubamura, H. *Nippon Kagaku Kaishi* **1980**, *3*, 1585.
(30) Harris, L. A. *J. Electrochem. Soc.* **1980**, *127*, 2657.
(31) González-Elipe, A. R.; Soria, J.; Munuera, G. *J. Catal.* **1982**, *76*, 254.

ductor surface, where subsequent reaction with surface oxygen species results in the detection of the target gas. In contrast, electronic sensitization involves the direct exchange of electrons between the semiconductor and the additive.[31] Electron density is transferred from the semiconductor to the additive, increasing the electron depletion layer in the semiconductor, leading to enhanced sensitivity upon the adsorption of a target gas.[2]

Previous studies on Ag−SnO_2 systems have shown a decrease in the Sn3d and O1s binding energies by 0.5−0.7 eV relative to those of pure SnO_2.[18,32] The shifts in binding energies reflected shifts in the Fermi energy of SnO_2 due to electronic interaction with the Ag additives. The electronic sensitization was responsible for the enhanced gas sensitivity in these systems. Studies on Pd−SnO_2 systems did not show shifts in the Sn3d and O1s binding energies relative to those of pure SnO_2.[17,32] The enhanced gas sensitivity of these systems was explained by a chemical interaction between SnO_2 and Pd.

XPS measurements were performed on 75% SnO_2−25% $InO_{1.5}$ doped with 0−10 wt % Pt and 2 wt % Au to elucidate the nature of interaction in these systems (Table 4). The nanocomposite with the optimal Au loading (2 wt %) displayed negligible binding energy shifts for the $Sn3d_{5/2}$ and $O1s_{1/2}$ peaks relative to the peaks for undoped 75% SnO_2−25% $InO_{1.5}$. For this system, the sensitivity to 1000 ppm CO (480) did not involve electronic interaction between Au and SnO_2−$InO_{1.5}$. It could be explained by a chemical interaction involving CO adsorption on Au, which has been known to be an excellent CO oxidation catalyst.[19]

For the Pt-doped nanocomposites, binding energy shifts were strongly influenced by the Pt loading (0−10 wt %) (Table 4). The 4 wt % Pt-doped nanocomposite, which possessed the highest sensitivity to 1000 ppm CO (6200), showed the largest shift in $Sn3d_{5/2}$ binding energies (ca. −0.7 eV), suggesting that the metal−semiconductor electronic interactions played an important role in the enhanced CO sensitivity.[19]

The 2 wt % Au-doped and 0−10 wt % Pt-doped nanocomposites calcined to 600 °C were found to exhibit no XRD peaks associated with metallic phases. This suggested that the metals were present as a highly dispersed phase.

TPD studies showed that the 75% SnO_2−25% $InO_{1.5}$ nanocomposite enhanced NO_x adsorption relative to that of pure SnO_2 and pure In_2O_3 (Figure 7), which was consistent with the higher NO_2 sensitivity of the 75% SnO_2−25% $InO_{1.5}$ nancomposite (6.0) compared with pure SnO_2 (1.2). The Al_2O_3-coated SnO_2 and Al_2O_3-coated 75% SnO_2−25% $InO_{1.5}$ adsorbed significantly more NO_x compared to pure SnO_2, with lower NO_x desorption peak temperatures. Their NO_x desorption peak temperatures (∼120 and 110 °C, respectively) corresponded well to their maximum NO_x sensitivity temperature of 150 °C. Thus, besides the ultrafine SnO_2 grain size (∼3 nm), the enhanced NO_x adsorption provided by both the Al_2O_3 coating and the secondary component (In_2O_3) contributed to the improved NO_x sensitivity of the 75% SnO_2−25% $InO_{1.5}$ nanocomposite.

(32) Matsushima, S.; Teraoka, Y.; Miura, N.; Yamazoe, N. *Jpn. J. Appl. Phys.* **1988**, *27*, 1798.

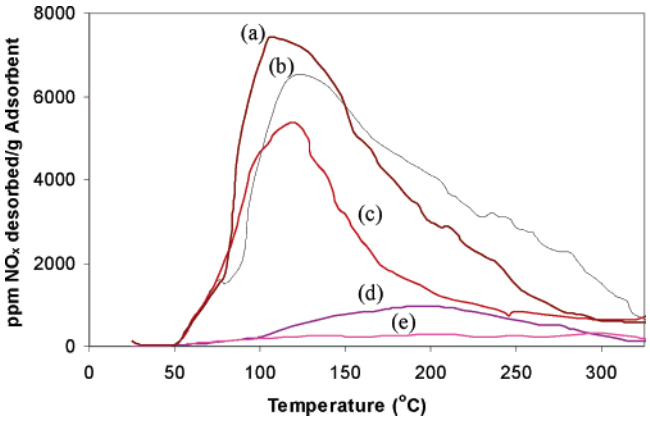

Figure 7. TPD of NO_x over (a) Al_2O_3-coated 75% SnO_2−25% $InO_{1.5}$, (b) Al_2O_3-coated SnO_2, (c) 75% SnO_2−25% $InO_{1.5}$, (d) pure SnO_2, and (e) pure In_2O_3. The samples were calcined to 600 °C; samples a and b contained 2 wt % Al.

Table 5. CO Sensitivity of 600 °C-Calcined SnO_2−$InO_{1.5}$ Nanocomposites Containing 2 wt % Pt or Al[a]

composition	additive modification method	CO sensitivity	NO_2 sensitivity	binding energy (eV), $Sn3d_{5/2}$
75% SnO_2−25% $InO_{1.5}$		11	6.0	487.0
2% Al, 75% SnO_2−25% $InO_{1.5}$	coating	7.0	1600	487.1
2% Pt, 75% SnO_2−25% $InO_{1.5}$	coating	19	7.1	487.0
2% Pt, 75% SnO_2−25% $InO_{1.5}$	doping	290	1.6	486.3

[a] The materials were exposed to 1000 ppm CO at 50 °C (CO sensitivity studies) and to 1 ppm NO_2 at 150 °C (NO_2 sensitivity studies). The uncertainty in the binding energy measurements was ±0.1 eV.

XPS studies were also used to show the effect of the modification method on the electronic interactions between the nanocomposite system (75% SnO_2−25% In_2O_3) and the metal additives (Table 5). The modification method had a dramatic impact on both the binding energy shifts of $Sn3d_{5/2}$ and CO sensitivity when Pt was used as an additive. When Pt was added as a dopant, a binding energy shift of −0.7 eV was noted, as well as a dramatic increase in CO sensitivity (290), compared to that of the unmodified 75% SnO_2−25% In_2O_3 composite (11). In contrast, when Pt was coated onto the nanocomposite, a binding energy shift was not observed compared to the binding energy of the unmodified nanocomposite, and CO sensitivity only increased slightly to 19. The results indicated the type of modification method (doping vs coating) had a dramatic effect on the electronic interactions and gas sensitivities of the nanocomposite system. Similar results were observed when a coating method was used to deposit Al_2O_3 onto the nanocomposite; there was a negligible shift in the $Sn3d_{5/2}$ binding energy. The use of the Al_2O_3 coating greatly increased NO_2 sensitivity, which was attributed to the enhanced chemical interaction between the NO_2 species and the Al_2O_3-coated nanocomposite, as shown by TPD studies (Figure 7).

4. Summary

Chemical precipitation of tin and indium chlorides was used to synthesize SnO_2−In_2O_3 nanocomposite powders possessing high thermal and phase stability compared to pure SnO_2 and In_2O_3. In particular, 75% SnO_2−25% $InO_{1.5}$ retained single-phase, ultrafine SnO_2 grains of ∼6 nm even after calcination at 800 °C. The nanocomposite system

demonstrated gas sensitivities significantly higher than those of conventional sensors based on pure SnO_2. In addition to serving as a grain growth inhibitor structurally, In_2O_3 provided for improved sensor performance via electronic interaction with the primary component, SnO_2. The $SnO_2-In_2O_3$ nanocomposite served as an excellent support material for the dispersion of noble metals and Al_2O_3 surface coatings, providing for further enhancements in selective gas adsorption and chemical/electronic synergistic effects. In particular, Au- and Pt-doped $SnO_2-InO_{1.5}$ displayed CO sensitivity superior to that of conventional Au- or Pt-doped SnO_2. The improved CO-sensing properties for Pt-doped $SnO_2-InO_{1.5}$ could be attributed to electronic sensitization effects of the noble metal. Highly sensitive NO_x sensors were also achieved with the Al_2O_3-coated $SnO_2-InO_{1.5}$ nanocomposite over a broad range of temperatures. The enhanced NO_x-sensing properties were attributed to increased NO_x adsorption.

Acknowledgment. This work was sponsored by the Office of Naval Research (Grant No. N00014-95-1-0626). J.T.M. acknowledges the support of a National Science Foundation Graduate Fellowship. We thank M. Frongillo for his assistance with the electron microscopy studies (MIT-NSF CMSE).

CM0617283